

15. Kecojevic, V. and Radomsky, M., Flyrock phenomena and area security in blasting-related accidents. *Saf. Sci.*, 2005, **43**(9), 739–750.
16. Little, T. N., Flyrock risk. Proceedings of EXPLO Conference, Wollongong, NSW, 3–4 September 2007, pp. 35–43.
17. Verakis, H. and Lobb, T., Flyrock revisited an ever present danger in mine blasting, 2007; <http://docs.isee.org/ISEE/Support/Proceed/General/07GENV1/07v109g.pdf>
18. Little, T. N. and Blair, D. P., Mechanistic Monte Carlo models for analysis of flyrock risk. *Rock Fragmentation by Blasting* (ed. Sanchidrián), Taylor & Francis, 2010, pp. 641–647.
19. Amini, H., Gholami, R., Monjezi, M., Torabi, S. R. and Zadhesh, J., Evaluation of flyrock phenomenon due to blasting operation by support vector machine. *Neural Comput. Appl.*, 2011, **21**(8), 2077–2085.
20. Ghasemi, E., Sari, M. and Ataei, M., Development of an empirical model for predicting the effects of controllable blasting parameters on flyrock distance in surface mines. *Int. J. Rock Mech. Min. Sci.*, 2012, **52**, 163–170.
21. Mishra, A. K. and Mallick, D. K., Analysis of blasting related accidents with emphasis on flyrock and its mitigation in surface mines. *Rock Fragmentation by Blasting* (eds Singh, P. K. and Sinha, A.), Taylor and Francis, London, 2013, pp. 555–561.
22. Lundborg, N., The hazards of fly rock in rock blasting. Swedish Detonic research foundation, Report DS, 1974, p. 12.
23. Roth, J. A., A model for the determination of flyrock range as a function of shot condition, US Department of Commerce, NTIS Report No. PB81222358, 1979, p. 61.
24. St George, J. D. and Gibson, M. F. L., Estimation of flyrock travel distances: a probabilistic approach, AusIMM EXPLO 2001 Conference, Hunter Valley, 2001, pp. 409–415.
25. McKenzie, C. K., *Flyrock Range and Fragment Size Prediction*, 2009; <http://docs.isee.org/ISEE/Support/Proceed/General/09GENV2/09v206g.pdf>
26. Monjezi, M., Bahrami, A. and Varjani, A. Y., Simultaneous prediction of fragmentation and flyrock in blasting operation using artificial neural networks. *Int. J. Rock Mech. Min. Sci.*, 2010, **47**, 476–480.
27. Stojadinović, S., Pantović, R. and Žikić, M., Prediction of flyrock trajectories for forensic applications using ballistic flight equations. *Int. J. Rock Mech. Min. Sci.*, 2011, **48**, 1086–1094.
28. Rezaei, M., Monjezi, M. and Varjani, Y. A., Development of a fuzzy model to predict flyrock in surface mining. *Saf. Sci.*, 2011, **49**, 298–305.
29. Ghasemi, E., Amini, H., Ataei, M. and Khalokakaei, R., Application of artificial intelligence techniques for predicting the flyrock distance caused by blasting operation. *Arab J. Geosci.*, 2012; doi:10.1007/s12517-012-0703-6, 10.
30. Monjezi, M., Dehghani, H., Singh, T. N., Sayadi, A. R. and Gholinejad, A., Application of TOPSIS method for selecting the most appropriate blast design. *Arab J. Geosci.*, 2012, **5**, 95–101.
31. Khandelwal, M. and Monjezi, M., Prediction of flyrock in open pit blasting operation using machine learning method. *Int. J. Min. Sci. Technol.*, 2013, **23**(3), 313–316.
32. Lilly, P. A., An empirical method of assessing rock mass blastability. Proceedings AusIMM/IE, Australian Newman Combined Group Large Open Pit Mines Conf., 1986, pp. 41–44, 89–92.

ACKNOWLEDGEMENTS. We thank Director, CSIR-CIMFR for permission to publish the paper. Thanks are due to Ministry of Mines (Govt of India) for partial funding. The work forms part of the Ph D thesis of the first author. Acknowledgement is due to the Indian School of Mines and other personnel for help.

Received 1 June 2015; revised accepted 22 June 2016

doi: 10.18520/cs/v111/i9/1524-1531

## New occurrence of albitite from Nubra valley, Ladakh: characterization from mineralogy and whole rock geochemistry

Aditya Kharya, H. K. Sachan\*, Sameer K. Tiwari, Saurabh Singhal, P. Chandra Singh, Santosh Rai, Sushil Kumar, Manish Mehta and P. K. R. Gautam

Wadia Institute of Himalayan Geology, Dehra Dun 248 001, India

**We report here the occurrence of albitite in Nubra valley of Ladakh region in the Trans-Himalaya area within Indian Territory at 34°44'46"N and 77°33'8"E before Panamik (in the Wish Pond, local name of the area). The albitite has been characterized by petrography, mineral chemistry, X-ray diffraction and whole rock geochemistry (i.e. major, trace and rare earth elements (REE)). The albitite comprises 85–96% albitite and amphibole, whereas apatite, zircon and ilmenite occur as accessory minerals. The textural relationship and geochemical data indicate its igneous origin. The albitite contains about 5–6 ppm U and Th which may possibly host U-REE mineralization.**

**Keywords:** Albitite, Karakoram, mineral chemistry, XRD, whole rock chemistry.

A number of albitite occurrences have been described in India within the Archaean basement and the Meso-Proterozoic cover rocks of Delhi Supergroup in north-central and northern Rajasthan<sup>1–3</sup>. Till now, there is only one known occurrence of albitite from Himalayan terrain, i.e. Swat valley of Pakistan in association with Mingora ophiolitic mélange<sup>4</sup>. However, such a rock type was not reported from Indian Himalayan or Trans-Himalayan region. Here, we present a detailed account of new occurrence of albitite from the Nubra valley of Shyok Suture Zone (SSZ) in trans-Himalayan region, based on petrography, XRD, mineral chemistry and whole rock geochemistry. The significance of albitite in Trans-Himalaya is important due to its peculiar occurrence in subduction-related tectonic setting (i.e. Shyok Suture Zone), whereas the albitites generally occur along the intercontinental rift zone<sup>1–3</sup>.

The SSZ is characterized as structural boundary which separates Ladakh magmatic arc in the south from the Karakoram terrain in the north. The SSZ runs parallel to Shyok river<sup>5</sup> (Figure 1). The Karakoram terrain contains a suite of rocks covering mélanges, ophiolites, sedimentary and metamorphic rocks. These rock sequences crop out in the Karakoram Range: the Nubra Formation<sup>6</sup>, the Karakoram leucogranite batholith (the Baltoro Plutonic Unit

\*For correspondence. (e-mail: hksachan@wihg.res.in)

in Pakistan), and an older I-type granitoid belt<sup>5</sup>. This granitoid belt runs parallel to Karakoram thrust. The area between Khalsar and Panamik mainly comprises varied lithologies including volcano-sedimentary sequences along with granites (Figure 1). These volcano-sedimentary sequences belong to the Nubra Formation. The Nubra Formation is a rock sequence c. 1–2 km wide cropping out along the foot of the Karakoram Range which occurs between the Tirit batholith and Karakoram leucogranite. This formation comprises gabbro, peridotite, serpentinite interbedded with phyllite, slate limestone,

and quartzites<sup>6</sup>. However, the occurrence of ultramafic rocks is unknown in this region<sup>7</sup>.

During the field work in Nubra valley in 2014, we found the pods of albitite within the metavolcanics (Figures 1 and 2). The host metavolcanics are metamorphosed up to greenschist facies. The metavolcanics consist of amphibole, epidote, albite, calcite, chlorite, quartz and Fe–Ti oxides, clinzoisite and Cr-spinel. The spinels mostly occur as subhedral to euhedral grains disseminated in the matrix of the other minerals. Epidote and clinzoisite are coarser-grained than other phases.

The albitite rock is characterized by petrography, XRD, mineral chemistry, whole rock chemistry (major, trace and rare earth elements (REE)). The albitite is a leucocratic, coarsely crystalline rock, which is hosted by metavolcanics in the Trans Himalaya. The overall texture of the rock is hypidiomorphic granular. The albitite rock mainly comprises albite, and amphibole; apatite, zircon and ilmenite occur as accessory minerals. Albite occupies 85–96 vol% of the albitite and is found as highly fractured coarse crystals (0.1–5 mm) grain size (Figure 3).

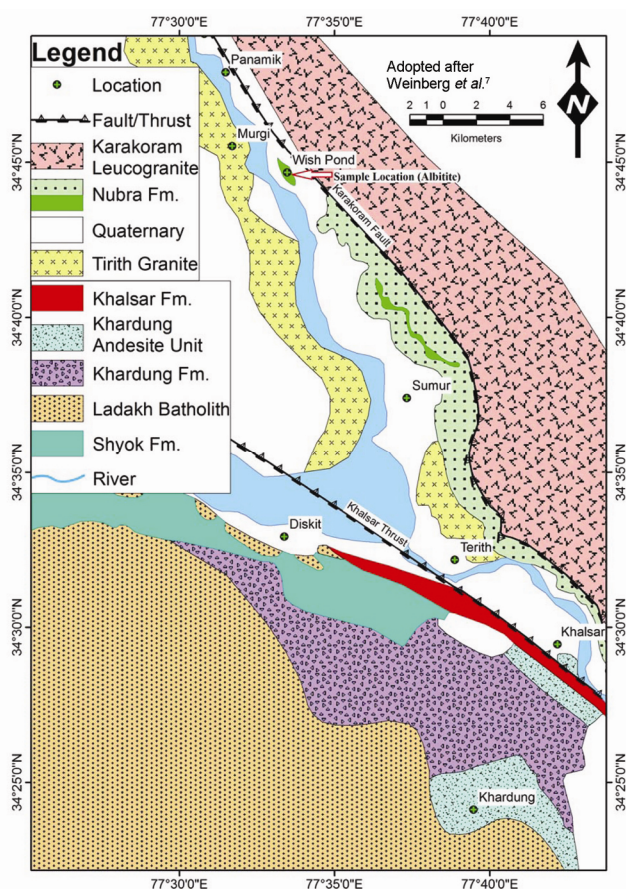


Figure 1. Geological map of the study area, showing the location of the studied sample (modified after Weinberg *et al.*)<sup>7</sup>.



Figure 2. Field photograph of Wish Pond and few sample locations on field.

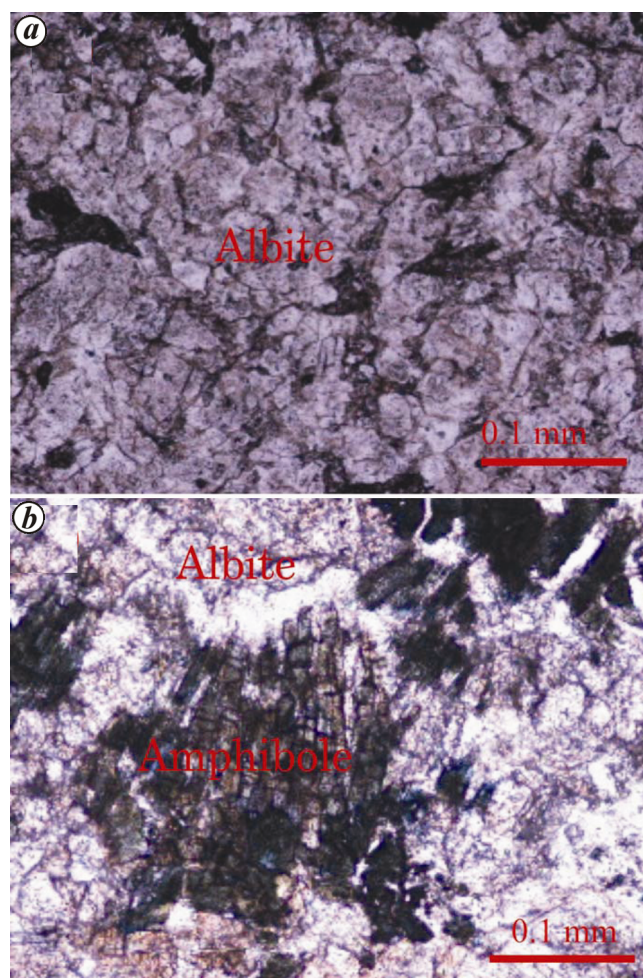


Figure 3. Photomicrograph showing (a) plagioclase (albite) grains and (b) plagioclase (albite) along with amphibole.



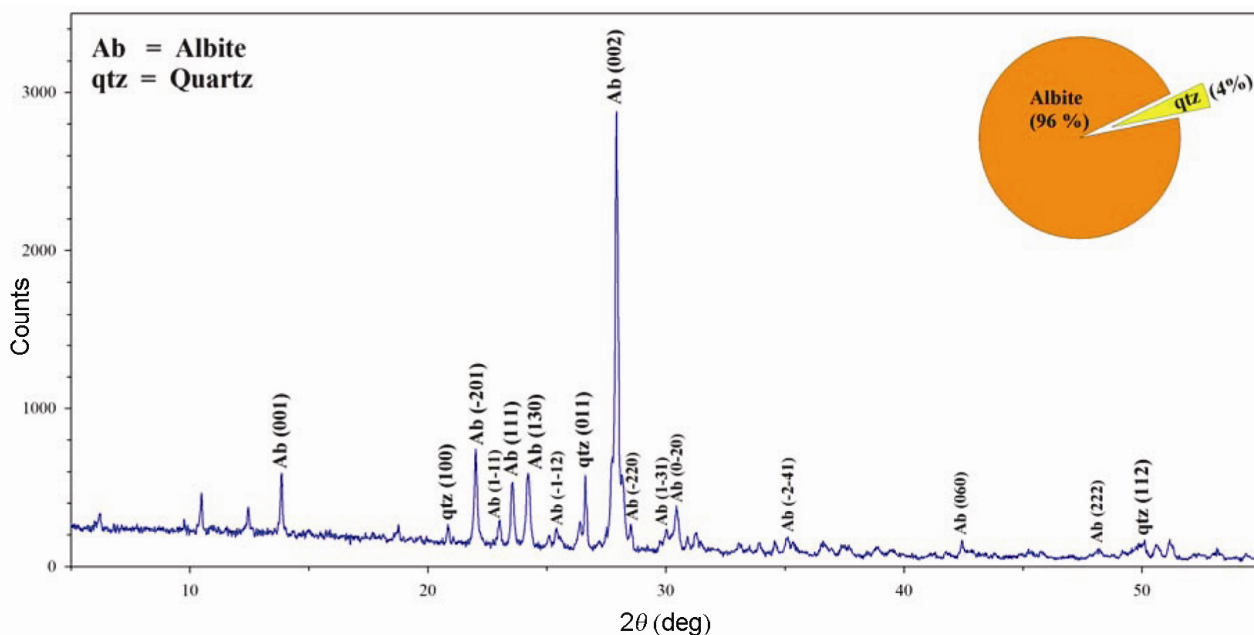


Figure 4. XRD pattern of albitite rock showing predominance of albite.

Table 1. Chemical composition of minerals present in albitite

	Albite		Titanite		Apatite		Amphibole	
SiO <sub>2</sub>	67.87	68.34	30.01	30.62	0.02	0.05	53.62	54.12
Al <sub>2</sub> O <sub>3</sub>	19.97	19.63	0.75	0.80	0.00	0.00	3.96	3.86
Na <sub>2</sub> O	11.37	11.67	0.02	0.00	0.00	0.00	1.96	1.89
P <sub>2</sub> O <sub>5</sub>	0.00	0.00	0.10	0.04	42.74	42.68	0.00	0.00
K <sub>2</sub> O	0.09	0.03	0.02	0.01	0.00	0.00	0.13	0.14
CaO	0.79	0.61	28.74	28.89	56.03	56.09	11.64	11.72
TiO <sub>2</sub>	0.03	0.00	38.14	37.55	0.03	0.00	0.28	0.23
Cr <sub>2</sub> O <sub>3</sub>	0.00	0.00	0.08	0.07	0.00	0.00	0.00	0.00
MnO	0.00	0.00	0.01	0.00	0.02	0.00	0.23	0.24
FeO	0.07	0.03	0.36	0.42	0.00	0.00	8.34	8.96
MgO	0.00	0.00	0.00	0.00	0.00	0.00	16.98	17.34
Sum:	100.19	100.31	98.23	98.40	98.84	98.82	97.14	98.76
Cations								
Si	2.966	2.981	3.997	4.066	0.003	0.008	7.632	7.603
Al	1.028	1.009	0.118	0.125	–	–	0.664	0.639
Na	0.963	0.987	0.005	–	–	–	0.225	0.197
P2	–	–	0.011	0.004	6.007	6.001	0.000	0.000
K	0.005	0.002	0.003	0.002	–	–	0.024	0.025
Ca	0.037	0.029	4.102	4.11	9.966	9.981	1.775	1.803
Ti	0.001	–	3.820	3.750	0.004	–	0.030	0.024
Cr	–	–	0.008	0.007	–	–	–	–
Mn	–	–	0.001	–	0.003	–	0.028	0.029
Fe <sup>2+</sup>	0.002	0.001	0.04	0.047	–	–	0.993	1.053
Mg	–	–	–	–	–	–	3.602	3.631
Or:	0.497	0.157	–	–	–	–	–	–
Ab:	95.832	97.041	–	–	–	–	–	–
An:	3.671	2.802	–	–	–	–	–	–

We carried out the XRD pattern on the sample using the diffractometer system XPERT-PRO at the Wadia Institute of Himalayan Geology (WIHG). The analytical condi-

tions are as follows. The start position ( $^{\circ}$ 2 $\theta$ .) was 2.0004 and end position was ( $^{\circ}$ 2 $\theta$ .) 79.9794. The step size ( $^{\circ}$ 2 $\theta$ .) was 0.0170 and scan step time (s) was

6.0800. The generator settings were 40 mA, 45 kV. The albitic nature of the studied sample was confirmed by XRD (Figure 4).

The mineral chemistry of various minerals in albitite is characterized by EPMA analyses at WIHG. The mineral analyses were obtained using a Cameca SX-100 electron microprobe. The operating conditions were 15 kV and 20 nA with a beam diameter of 1 µm. Natural mineral samples were used for calibration, except that synthetic oxides were used for Mn and Ti. The PAP correction was applied using software provided with the electron microprobe.

The albite (Ab<sub>97</sub>An<sub>2</sub>Or<sub>1</sub>) occurs as large euhedral to subhedral crystals, archetypally with oscillatory zoning. It displays plastic deformation fabrics such as kink bands and undulatory extinction, and later undergoes brittle fragmentation. Chemical analysis of euhedral plagioclase does not show a large compositional range. The Na contents range from 11.37% to 11.67%. The Ca and Fe vary between 0.61% and 0.79% and 0.3% to 0.7% respectively. This composition can be construed in two ways. First, direct crystallization from Na-rich magma could have occurred<sup>8</sup>. Second, a primary zoned plagioclase could have changed to albite by metasomatism<sup>9</sup>.

The albitites contain as much as 3 vol% apatite. Apatite occurs as large subhedral grains, and is commonly highly fractured. Large apatite grains exhibit high concentration of Ca and P content respectively. The Ca varies between 56.01% and 56.07%, whereas P varies from 42.68% to 42.74%. All other elements are present in negligible content (Table 1). Titanite occurs as large anhedral grains. It contains Ca between 28.74% and 28.89%, whereas Ti shows variation between 37.55% and 38.14% (Table 1). Ca-bearing plagioclase is the only source of Ca in titanite, and the titanite is the reaction product of Ca-bearing plagioclase with ilmenite<sup>10</sup>. The representative analyses of amphibole are given in Table 1. Amphiboles are rich in Ca and Mg, which vary between 11.34% to 11.98% and 16.98% to 17.34% respectively. According to the classification of amphiboles by Leake *et al.*<sup>11</sup>, the amphiboles are classified as actinolite,

Major and trace elements were analysed at WIHG by WD-XRF (Bruker Tiger S8) following the procedure of Saini *et al.*<sup>12</sup>. REE were analysed using ICP-MS (Perkin Elmer, ELAN DRC-e) following the procedure of Khanna *et al.*<sup>13</sup>.

The whole rock analyses of the albitite sample show that these rocks contain large amounts of SiO<sub>2</sub> (63.38 wt%), Al<sub>2</sub>O<sub>3</sub> (16.69 wt%), CaO (5.27 wt%), MgO (1.97 wt%) and Na<sub>2</sub>O (8.01 wt%) (Table 2). The Sr and Zr concentration in the studied sample is relatively higher (i.e. 324 and 214 ppm respectively) whereas U and Th concentrations vary between 5 and 6 ppm. The albitite sample (HAL) shows similarities in its REE concentration, especially in MREE and HREE with SAL (Slavezines massif albitite)<sup>14</sup>, and Central Sardinia, Italy, albitite<sup>15</sup> and

Malakwa albitite<sup>16</sup>, while LREE (La to Nd) concentration is slightly different from other albitites (Table 2). The studied sample of albitite shows Eu negative anomaly which may relate to original Eu anomalies in the albitite protolith. Similar REE patterns with Eu<sup>-</sup> (negative) anomalies were recorded in SAL from France and albitite deposits from central Sardinia (CAL), Italy<sup>14,15</sup>. The

**Table 2.** Comparative study of major, trace and REE composition of albitite samples

	MI5	SAL 03-17	CAL	W14A
Oxide (wt%)				
SiO <sub>2</sub>	65.00	64.63	68.52	63.38
TiO <sub>2</sub>	0.01	0.01	0.18	0.85
Al <sub>2</sub> O <sub>3</sub>	19.16	20.74	18.70	16.69
Fe <sub>2</sub> O <sub>3</sub>	0.03	0.34	0.11	0.66
MnO	0.01	0.01	0.01	0.02
MgO	0.02	0.37	0.03	1.97
CaO	0.95	0.90	1.87	5.27
Na <sub>2</sub> O	9.70	9.45	10.30	8.01
K <sub>2</sub> O	0.06	1.22	0.14	0.24
P <sub>2</sub> O <sub>5</sub>	0.04	0.20	0.01	0.36
BaO	0.03	1.29	0.24	nd
SrO	0.05	nd	nd	nd
LOI	0.00	nd	nd	1.47
Total	100.06	99.10	100.01	98.92
A/NK (molar)	1.20			
A/CNK (molar)	1.07			
Trace (ppm)				
Cr	8.00	9.26	nd	25.00
Ni	4.00	nd	nd	21.00
Co	2.00	0.21	nd	nd
Zn	1.00	1.57	nd	17.00
Sc	7.00	nd	nd	14.20
Ga	9.00	17.70	nd	17.00
V	7.00	nd	10.00	70.00
Pb	10.00	3.24	nd	16.00
Yb	2.00	0.07	nd	nd
U	0.01	0.52	1.40	5.40
Th	14.00	0.48	57.90	6.00
Hf	1.00	0.04	nd	nd
REE (ppm)				
La	42.00	0.69	82.70	1.949
Ce	70.00	1.83	198.00	5.944
Pr	5.00	0.23	23.00	1.126
Nd	13.00	0.97	87.60	6.545
Sm	2.00	0.23	14.50	2.441
Eu	0.20	0.06	1.10	0.418
Gd	3.00	0.22	6.10	2.331
Tb	0.30	0.03	0.60	0.537
Dy	2.00	0.16	2.70	3.465
Ho	1.00	0.02	0.50	0.773
Er	1.40	0.08	1.40	2.189
Tm	0.23	0.01	0.30	0.318
Yb	1.40	0.07	1.20	1.795
Lu	0.20	0.01	0.30	0.2260

After Boulvais *et al.*<sup>14</sup>; Castorina *et al.*<sup>15</sup>. LOI, Loss of ignition; REE, rare earth elements; nd, no data. MI5, Malakwa albitite; SAL 03-17, Slavezines massif, France, albitite; CAL, Central Sardinia, Italy, albitite; W14A, Wish pond albitite (studied sample).

A/CNK [A/CNK =  $\text{Al}_2\text{O}_3/(\text{CaO} + \text{Na}_2\text{O} + \text{K}_2\text{O})$ ] ratio of studied sample is 1.20 and A/NK [A/NK =  $\text{Al}_2\text{O}_3/(\text{Na}_2\text{O} + \text{K}_2\text{O})$ ] ratio is 1.07 which shows close relationship to the peraluminous field according to the criteria of Shand<sup>17</sup> and tends to be Al-saturated with an A/CNK ratio close to 1, which is the value of albite. The  $\text{SiO}_2/\text{Al}_2\text{O}_3$  ratio of studied sample is 3.81. A comparison of this ratio along with A/CNK indicates its relation to trondjemite according to the criteria of Kaur and Mehta<sup>18</sup>. The studied sample from Nubra has  $(\text{Na}_2\text{O} + \text{K}_2\text{O})\%$  concentration of 8.25%. The concentration of  $(\text{Na}_2\text{O} + \text{K}_2\text{O})\%$  versus  $\text{SiO}_2$  according to Miyashiro<sup>19</sup> indicates the alkaline nature of the albitite. The alkalic or sodic affinity reveals that the magmatic process leading to formation of albitite was intraplate in nature<sup>20</sup>.

The  $\text{SiO}_2$ ,  $\text{Al}_2\text{O}_3$  and  $\text{Na}_2\text{O}$  contents of the studied sample are very much similar to Rajasthan albitite line<sup>1</sup>, whereas CaO content is slightly enriched in comparison to Rajasthan albitites. It might be possible that Nubra albitite may have some affinity with continental rift environment but the field setting of the studied sample does not corroborate such a tectonic environment.

The geochemical data and textures preserved in the albitite sample indicate that the protolith of Nubra albitite was igneous in origin. Furthermore, the intimate association with ultramafic rocks of the ophiolitic metavolcanics suite suggests a plagiogranite origin for the albitites. The possibility that the Nubra albitite originated from Na-rich magma may be invoked. However, the lack of Na-rich igneous rocks in the ultramafic suite rules out this possibility.

The concentration of uranium in the studied sample is between 5 and 6 ppm. It is a worldwide phenomena that the uranium deposits frequently occurs in soda-rich rocks (i.e. albitite). The significance of this new albitite occurrence in Himalayan terrain may be related to possible uranium-REE mineralization, which may open new vistas for its exploration.

valleys, Northern Ladakh: Linking Kohistan to Tibet. *Tectonics of the Nanga Parbat Syntaxis and the Western Himalaya*, 2000, **170**, 253–275.

8. Schwartz, M. O., Geochemical criteria for distinguishing magmatic and metasomatic albite-enrichment in granitoids – examples from the Ta-Li granite Yichun (China) and the Sn-W deposit tikus (Indonesia). *Miner. Deposita*, 1992, **27**, 101–108.
9. Smith, J. V., Feldspar minerals. Tom 2. *Chemical and Textural Properties*, Springer-Verlag, Berlin, 1974.
10. Harlov, D., Tropper, P., Seifert, W., Nijland, T. and Förster, H.-J., Formation of al-rich titanite (catissio 4 o-caalsio 4 oh) reaction rims on ilmenite in metamorphic rocks as a function of  $f_{\text{H}_2\text{O}}$  and  $f_{\text{O}_2}$ . *Lithos*, 2006, **88**, 72–84.
11. Leake, B., Nomenclature of amphiboles: report of the subcommittee on amphiboles of the international mineralogical association, commission on new minerals and mineral names. *Can. Mineral.*, 1997, **35**, 219–246.
12. Saini, N., Mukherjee, P., Rathi, M., Khanna, P. and Purohit, K., A new geochemical reference sample of granite (dg-h) from Dalhousie, Himachal Himalaya. *Geol. Soc. India*, 1998, **52**, 603–606.
13. Khanna, P. P., Saini, N. K., Mukherjee, P. K. and Purohit, K. K., An appraisal of icp-ms technique for determination of rees: Long term qc assessment of silicate rock analysis. *Himal. Geol.*, 2009, **30**, 95–99.
14. Boulvais, P., Ruffet, G., Cornichet, J. and Mermet, M., Cretaceous albitization and dequartzification of hercynian peraluminous granite in the salvezines massif (French pyrénées). *Lithos*, 2007, **93**, 89–106.
15. Castorina, F., Masi, U., Padalino, G. and Palomba, M., Constraints from geochemistry and Sr–Nd isotopes for the origin of albitite deposits from Central Sardinia (Italy). *Miner. Deposita*, 2006, **41**, 323–338.
16. Mohammad, Y. O., Maekawa, H. and Lawa, F. A., Mineralogy and origin of mlakawa albitite from Kurdistan region, Northeastern Iraq. *Geosphere*, 2007, **3**, 624–645.
17. Shand, S. J., *Eruptive Rocks: Their Genesis, Composition*, John Wiley, New York, 1943.
18. Kaur, G. and Mehta, P., The gothara plagiogranite: evidence for oceanic magmatism in a non-ophiolitic association, north Khetri copper belt, Rajasthan, India? *J. Asian Earth Sci.*, 2005, **25**, 805–819.
19. Miyashiro, A., Nature of alkalic volcanic rock series. *Contrib. Mineral. Petrol.*, 1978, **66**, 91–104.
20. Le Bas, M., Ultra-alkaline magmatism with or without rifting. *Tectonophysics*, 1987, **143**, 75–84.

1. Ray, S. K., The albitite line of northern rajasthan – a fossil intracontinental rift-zone. *J. Geol. Soc. India*, 1990, **36**, 413–423.
2. Fareedudin and Bose, U., A new occurrence of albitite dyke near Arath, Nagaur district, Rajasthan. *Curr. Sci.*, 1992, **62**, 635–636.
3. Yadav, G. S., Muthamilselvan, A., Shaji, T. S., Nanda, L. K. and Rai, A. K., Recognition of a new albitite zone in northern Rajasthan: its implications on uranium mineralization. *Curr. Sci.*, 2015, **108**, 1994–1998.
4. Barbier, M., Caggianelli, A., Di Florio, M. and Lorenzoni, S., Plagiogranites and gabbroic rocks from the mingora ophiolitic mélange, swat valley, NW Frontier Province, Pakistan. *Mineral. Mag.*, 1994, **58**, 553–566.
5. Srimal, N., India-asia collision: implications from the geology of the eastern Karakoram. *Geology*, 1986, **14**, 523–527.
6. Thakur, V. and Misra, D., Tectonic framework of the Indus and Shyok suture zones in Eastern Ladakh, Northwest Himalaya. *Tectonophysics*, 1984, **101**, 207–220.
7. Weinberg, R. F., Dunlap, W. J. and Whitehouse, M., New field, structural and geochronological data from the Shyok and Nubra

ACKNOWLEDGEMENT. We gratefully acknowledge Prof A. K. Gupta, Director, WIHG for his constant encouragement and his kind permission to publish the paper.

Received 25 February 2016; revised accepted 7 July 2016

doi: 10.18520/cs/v111/i9/1531-1535